Evaluation of Land Cover Change and Agricultural Protection Sites: A GIS and Remote Sensing Approach for Ho Chi Minh City, Vietnam

Mathias Schaefer [*], Nguyen Xuan Thinh

TU Dortmund University, Department of Spatial Information Management and Modelling, 44227, Dortmund, Germany

ABSTRACT

Ho Chi Minh City (HCMC), economic center and most populous city of Vietnam faces a strong structural change since its market liberalization in the late 1980s. Big challenges occur in the form of uncontrolled urban sprawl due to rapid population growth with encroachment of agricultural land, which leads to environmental and climatic issues like urban heat island effects, air pollution and flooding events. Remote Sensing and Geographic Information Systems (GIS) provide new computer-based technologies for urban planners which can greatly ease the monitoring of agricultural loss as well as improve decision making for future land management. In the first part of this study, land cover change dynamics are thoroughly assessed using moderate and high spatial resolution satellite imagery (Landsat and SPOT) over the period 2010–2017 in 22 districts of HCMC. In the second part, the land cover classification results of 2017 provide the initial map for a GIS-based Multi-Criteria-Decision-Analysis (MCDA) of potential agricultural protection sites. Therefore, criteria of climate adaptation and ecological service are established and embedded in the GIS-compatible Compromise Programming Model (CP). With the use of Analytic Hierarchy Process (AHP) by Thomas L. Saaty and additional expert knowledge, appropriate weighting factors have been affiliated. The results show that agricultural land decreased by more than two thirds in the period considered. However, particularly the western rural districts Bình Chánh and Hóc Môn still offer a great amount of valuable agricultural land suitable for protection. The proposed method can serve as a scientific framework for planning departments of fast growing cities to zone agricultural land for protection on an early planning stage in order to ensure sustainable land use development in the future.

1. Introduction

Vietnam has undergone significant structural changes over the past decades. Through a series of Reforms (Vietnamese: Đổi mới) in the late 1980s, the central planned economy has been switched to a market-oriented, liberal economic policy. Trade relations with western countries were expanded and foreign direct investments (FDI) were given high priority. To strengthen the incentive for foreign investors, local governments opted for tax breaks. Ten years after the reform, foreign companies already accounted for 13% of Vietnam's Gross Domestic Product (GDP) (Kontgis et al., 2014). Consequently, the rapid economic growth created a wave of land conversion in favor of industrial commercial sites. New jobs in the secondary sector resulted in strong population growth and new construction activity (McGee, 2002).

An illustrative example of this rapid development can be observed in Ho Chi Minh City (until 1975 Saigon, hereinafter HCMC), located in southern Vietnam north to the Mekong Delta. Since the mid-2000s,

uncontrolled decentralization processes have dominated the city's agricultural periphery due to ongoing population growth (Kontgis et al., 2014). Between 2000 and 2010, agricultural area decreased by 6%. Simultaneous, the share of new residential area increased by 7% (Downes et al., 2016). Moreover, the number of agricultural households has been reduced to one sixth in comparison to 1997. In this context, agriculture also plays an existential role for many family farms in HCMC, as the loss of 1ha of agricultural land also implies a loss of 13 jobs (Vu and Kawashima, 2017). From a macroeconomic perspective, the cultivation of rice, fruits, vegetables and grains is important for a stable economy (Rutten et al., 2014). Ultimately, uncontrolled land conversion also entails climate disaster risks, especially because HCMC ranked sixth among the cities most vulnerable to climate change 2013 (Maplecroft, 2012). In total, 70% of settlement areas in HCMC lies below two meters above mean sea level (Downes et al., 2016). The combination of tropical climate, shallow topography and uncontrolled urbanization leads to an inadequate flood retention in riverside districts (Storch and Downes,
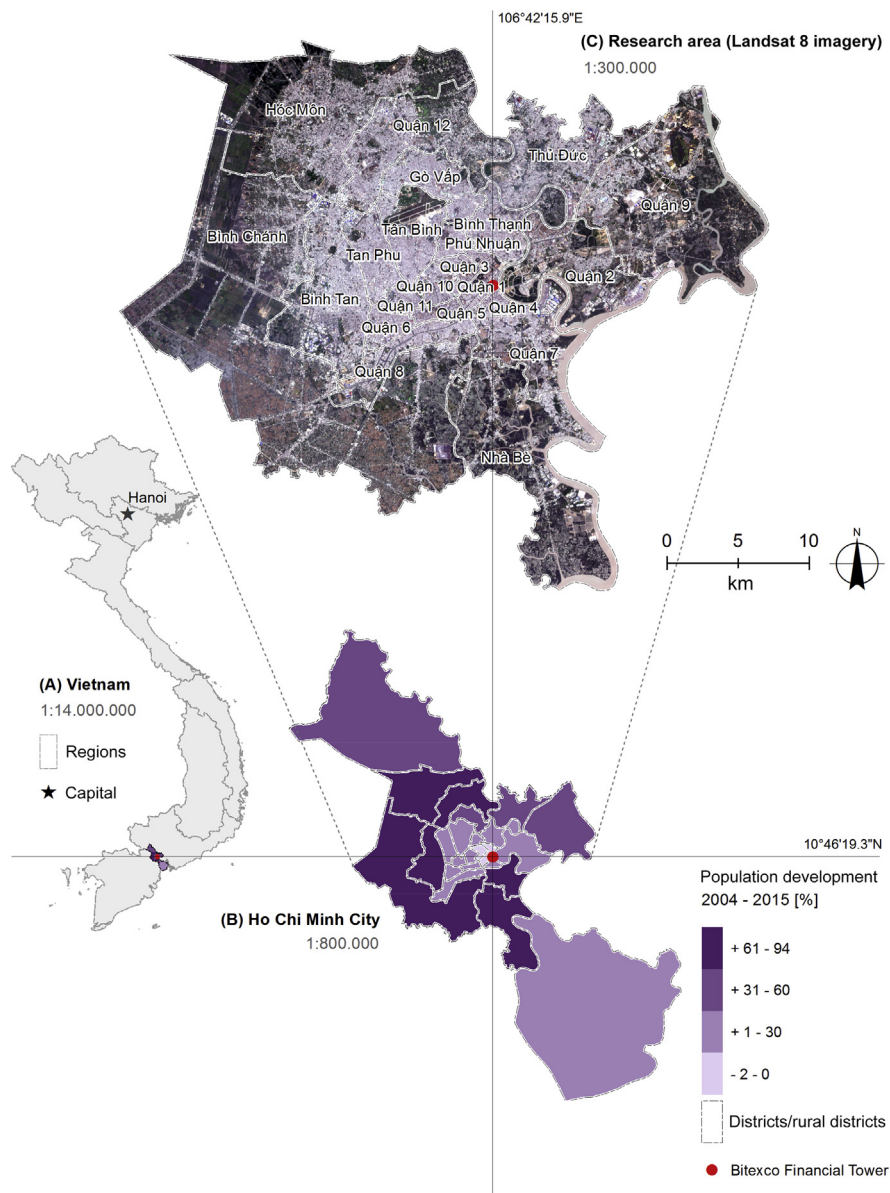
Fig. 1. Geographical location of the study area.

2011; Nguyen et al., 2016). At the same time, dense construction without ventilation fosters urban heat island effects, which can lead to an increased mortality rate, especially among old and diseased residents (Katzschner and Burghardt, 2013; Son et al., 2017). The mentioned developments point to a trend where agriculture with its ecological, social and economic value has been given lower priority to the sealing process. There is an increasing need for local planning authorities to enhance the monitoring of land conversion as well as to protect agricultural land in order to ensure flooding retention sites and fresh air production zones (Li and Yeh, 2001; Gravert and Wiechmann, 2016).

GIS and satellite-based image analysis can be used as established instruments of urban and environmental planning to visualize and understand changes in landscape and spatial relationships (Piekarczyk, 2014). For example, Remote Sensing imagery can provide up-to-date land cover information, which is a cost-effective way for fast-growing cities like HCMC, as traditional mapping is often time-consuming and digital data about land use in Vietnam is often sparse (Giri, 2012; Vu et al., 2018). Furthermore, remotely sensed data like Landsat imagery is freely available online and covers almost the whole earth, which allows continuous monitoring of land cover change since 1972 (USGS, 2013). On the other hand, GIS are particularly suitable for the computer-based analysis of geometric forms of a certain land use like compactness and contiguity. Through their combination, both disciplines can benefit from each other (AbdelRahman et al., 2016).

Likewise, the selection of agricultural areas suitable for protection should be based on a transparent method according to reliable criteria and indicators in order to guarantee the replicability of the results. Typically, the optimal solution of a perfect landscape arrangement which corresponds to the preferences of all decision-makers is utopian, because of potential conflicts of use, restrictions on nature or legal regulations. This assumes to well structure the decision problem and differentiate between various solutions to identify the most preferred alternatives. With the use of a Multi-Criteria-Decision-Analysis (MCDA), a compromise solution can be created. Here, alternatives (e.g. agricultural areas) are assessed based on quantitatively measurable indicators. The final choice of alternatives depends on their degree of suitability achievement indicating to what extent the characteristic values of a certain indicator correspond to the main objective (Malczewski, 2004). Representatives of this type of MCDA are called Multi-Attributive-Decision-Analysis (MADA) like the Analytic Hierarchy Process (AHP) by Thomas L. Saaty

Table 1
Data used.

	Data	Date of Acquisition	Spatial resolution/Scale	Source
Remote Sensing	Landsat 5 TM	11/02/2010	30 m × 30 m	United States Geological Survey (USGS)
Satellite Images	Landsat 8 OLI TIRS	14/02/2017	30 m × 30 m	
	SPOT 5 mosaic	14/02/2015	2.5 m × 2.5 m	AIRBUS Defence and Space
GIS data	Digital Elevation Model (DEM)	2010	5 m × 5 m	DoNRE
	Land use map	2010	1:5.000	
	Administrative boundaries	2015	1:10.000	Global Administrative Areas, www.gadm.org

and the Compromise Programming (CP) method by Milan Zeleny (Zeleny, 1976; Saaty, 2008; Yalew et al., 2016). The implementation of both methods into a GIS environment has been extensively exploited to solve complex decision problems like site assessments for urban agriculture, rice cultivation or new urban settlements (Pham, 1999; Malczewski, 2004; Marinoni, 2004; Thinh et al., 2004; Kihoro et al., 2013; La Rosa et al., 2014; Yalew et al., 2016).

This leads to the main objective of a GIS and Remote Sensing-based evaluation of agricultural land in terms of their structural change and potential of future protection in HCMC. In the first part of this study, two land cover maps will be generated with the use of Remote Sensing techniques and pixel-based supervised classification algorithm. Subsequently, a change detection analysis should visualize, how the landscape in HCMC has transformed over the time period from 2010 und 2017. The second part is based on a MCDA, in which existing agricultural areas from the year 2017 are tested for different climatic and environmental functions and weighed against each other regarding their equivalent protective suitability. Finally, the results will be brought into a decision making context, in order to prevent agricultural land from further fragmentation processes.

2. Study area and data

With over eight million inhabitants and a GDP of approximately $128 billion in 2015, HCMC is the most populous city and economic center of Vietnam (Statistical Office HCMC, 2015a). Agriculture has a long tradition in this region as surrounding marshes provide fertile soils for different crops. The predominant crops cultivated in HCMC are rice, corn, wheat, tea, coffee, rubber, spices, fruits and other vegetables (Statistical Office HCMC, 2015b). In the southern part of the city, fish- and shrimp-farming becomes more important as they tend to be a better source of income. HCMC is divided into 19 urban districts (Quận) and 5 rural districts (Huyện). The actual study area extends to all 19 urban districts and to 3 rural districts[1] (Fig. 1). These 22 districts accumulated have a size of 956.6 km^2 and are home to approximately 7.770.000 inhabitants in 2015, corresponding to 94% of the city's total population (Statistical Office HCMC, 2015a). Census data show that especially the rural districts Hóc Môn, Bình Chánh, Bình Tân and Nhà Bè have undergone a significant population growth during a period of 10 years (2005–2015). The ongoing population growth also correlates to new housing projects from 2006 to 2009 converting farmland into urban settlements (Hirsch, 2017; Goldblatt et al., 2018). In the southern Quận 7, new urban development was implemented since the late 1990s (Vu et al., 2018). As a matter of fact, Quận 4 in the south became an important connection part between Quận 7 and the other urban core districts. Since the establishment of new infrastructure such as the underwater Saigon Tunnel in 2011, new construction activities and an increasing number of inhabitants can also be observed in Quận 2 (Statistical Office HCMC, 2015a). For instance, the new construction project

Thủ Thiêm adjoining the Saigon River can be mentioned, which should replace Quận 1 as Central Business District in the future (HARMS, 2013).

Since 1993, different construction plans for HCMC do exist, which specify the urban development for the future. Unfortunately, each of these plans is currently in force and there is little consensus on major development directions due to their overlapping (Du, 2015). Furthermore, the Vietnamese government passed a resolution on the adaptation of land use in HCMC. In this decision, it was approved that HCMC may convert 26.246ha of agricultural land for non-agricultural purposes, e.g. into industrial, commercial and/or residential areas in the period 2016–2020 (Vietnam National Assembly, 2017).

For this study, Landsat images with 30m spatial resolution were acquired from free available USGS Earth Explorer online archive. The initial year of analysis should be 2010 in order to compare the classification results with the official land use map provided by HCMC Department of Natural Resources and Environment (DoNRE). For 2010, two Landsat 5 Thematic Mapper (TM) were needed to cover the whole study area. A single scene of Landsat 8 Operational Land Imager (OLI) and Thermal Infrared Sensor (TIRS) acquired on 14/02/2017 was used for 2017. Because there has not been enough cloud free data for multiseasonal imagery classification, this study assumes a single date classification for both years. However, the acquired imagery was taken in the same growing season, so a comparability is ensured (Dutta et al., 1998). A SPOT 5 mosaic with a 2,5m resolution, Google Earth and an official land use map of HCMC served as reference data for better object identification (Table 1). All images contained no clouds covering the study area. Compared to a 2-dimensional representation of satellite images or land use maps, the supplied Digital Elevation Model (DEM) represents the vertical extent of the study area's surface by height values per pixel. Buildings and vegetation are not included in this model.

3. Methods

3.1. Pre-processing and field survey

The pre-processing of the satellite images was performed using ENVI 5.1 software (Exelis Visual Information Solutions) in order to extract land cover information as efficiently as possible. Dark Object Subtraction (DOS) algorithm was used on all Landsat images to remove atmospheric scattering effects like dust and haze but also to sharpen the contrast between land covers (Gilmore et al., 2015). The transformation from digital grey numbers to reflectance values is an automated process in ENVI by using the sourced Landsat metadata. As a last step, the two Landsat 5 TM scenes for 2010 were mosaicked into a single image. The supplied geodata and the pre-processed imagery were projected into the Universal Transverse Mercator coordinate system (UTM) zone 48 north and clipped to the study area. This coordinate system was also used for the whole research. The analysis of the geodata was based on ArcGIS for Desktop Advanced 10.4.1 (Environmental Systems Research Institute, ESRI) and its Spatial Analyst extension.

In Addition, 60 georeferenced ground truth points with precision of ±5m were gathered during a field survey between 13/03/2017 and 18/03/2017 using code-based Leica Zeno 20 GPS Handheld Computer. Correspondingly, photographs of different land cover types were taken and geo-tagged to the collected ground truth points in ArcGIS.

---

[1] The southern district Cần Giờ won't be considered, since almost the entire area is covered by protective mangrove forests and thus irrelevant to the research objective. Nevertheless, the northern rural district Củ Chi is excluded from the analysis, since a large area is not covered by the high-resolution SPOT 5 mosaic as the basis for the accuracy analysis of the classification.

3.2. Land cover classification and accuracy assessment

Since the multi-temporal comparison of the same area through satellite imagery is possible, change detection analysis of natural and artificial surfaces in Vietnam is well established (Rowcroft, 2008; Disperati and Virdis, 2015; Tran et al., 2015; Laux et al., 2017). Other studies have also demonstrated that satellite imagery is adequate for land cover change detection in HCMC (van Tran and Ha, 2007). The benefit for spatial planning lies in the possibility to show an up-to-date spatial distribution of agricultural areas as well as to identify the main driving forces for agricultural loss in HCMC.

In order to carry out the digital change detection and to locate agricultural land suitable for protection, data about the current and past land cover in HCMC is needed. For this reason, the prepared and calibrated satellite data for 2010 and 2017 was undergone a pixel-based supervised classification. Therefore, eight separate land cover classes[2] were carried out to define the landscape in the study area:

1. *Built up areas* (residential buildings, industrial use, roads, villages, other impervious surfaces)
2. *Rice paddy*
3. *Annual plants* (maize, millet, wheat, sugar-cane, other vegetables)
4. *Perennial plants* (tea, coffee, rubber, orange, lemon, banana and cinnamon)
5. *Forests* (forestry, natural forests, individual trees, mangroves)
6. *Lower vegetation* (abandoned agricultural land, grass, pastures, shrubs)
7. *Bare soils* (fallow land, sands, earth dumps)
8. *Water bodies* (rivers, canals, lakes, artificial ponds)

The three classes focusing on agriculture (rice paddy, annual plants and perennial plants) are based on the terminology of the Department of Natural Resources and Environment (DoNRE) and the Statistical Office HCMC (Statistical Office HCMC, 2015b). Furthermore, the detailed classification of agriculture allows a finer distinction of potential changes. However, because of the medium resolution of Landsat imagery and the fine river networks in the south of the study area, no satisfactory pixel-based distinction can be made between natural and artificial water bodies like aquaculture ponds (Zhang et al., 2010; Ottinger et al., 2017, 2018).

False color composite, Normalized Difference Vegetation Index (*NDVI*) as well as the Modified Soil Adjusted Vegetation Index 2 (*MSAVI$_2$*) by Qi et al. were calculated for vegetation extraction and distinguishing between different agricultural uses (Qi et al., 1994):

$$NDVI = \frac{NIR - R}{NIR + R} \qquad (1)$$

$$MSAVI_2 = \frac{1}{2}\left[2*NIR + 1 - \sqrt{(2*NIR + 1)^2 - 8*(NIR - R)}\right] \qquad (2)$$

whereby NIR (Near Infrared) is band 5 of Landsat 8 (band 4 of Landsat 5) and R (Red) is band 4 of Landsat 8 (band 3 of Landsat 5). The Modified Normalized Difference Water Index (*MNDWI*) by Xu helped for detection and masking of water bodies (Xu, 2006):

$$MNDWI = \frac{G - SWIR}{G + SWIR} \qquad (3)$$

whereby G (Green) is band 3 of Landsat 8 (band 2 of Landsat 5) and SWIR

---

[2] Satellite imagery analysis only allows to map the physical characteristics of earth. Land *cover* describes the biophysical state of the earth's surface in case of the natural environment (e.g. vegetation or water) including artificial structures such as buildings. Land *use* refers to the anthropogenic purpose for which land is designated Turner et al. (1995).

(Short Wave Infrared) is band 6 of Landsat 8 (band 5 of Landsat 5). All spectral bands of Landsat imagery (2010 and 2017) have undergone a Tasseled Cap Transformation to compress the most spectral information into three bands (Kauth and Thomas, 1976; Crist and Cicone, 1984; Baig et al., 2014). For the creation of the two land cover maps, Maximum Likelihood Classifier (MLC) in ENVI 5.1 was applied to a layer stack of MSAVI and multispectral bands (Ahmad and Quegan, 2012). The training sites for each land cover class were selected through visual interpretation of the Landsat scenes, Google Earth, SPOT5 mosaic, in situ images and the official land use map of 2010. According to McCoy, seven training samples with a minimum size of ten pixels were selected for each class (McCoy, 2005).

In order to figure out whether the results meet the requirements for post-classification comparison and further analysis, it is necessary to perform an accuracy assessment. To assess the accuracy, statistical parameters such as overall accuracy (O$_A$), Kappa coefficient (k), user (U$_A$) and producer accuracies (P$_A$) were computed using 208 random sampled ground truth points (28 points per class) for both years (Brennan and Prediger, 1981; Fitzpatrick-Lins, 1981; Congalton and Green, 2009).

3.3. Criteria and indicators for agricultural protection sites

A total of six indicators were derived, which are related to climate adaptation criteria (*Cold air production* and *Flood retention*) as well as ecological criteria (preservation of green belts). GIS raster maps on the six indicators were calculated, while each grid cell was evaluated for suitability of agricultural protection. The raster cell size was resampled to the resolution of the supplied DEM (5 m × 5 m) in order to attain the maximum detailed results as possible. Four stages of protection suitability were divided into highly, rather, marginally and not suitable for protection. At this point, it is important to standardize the heterogeneous input dataset into comparable units between 0 (least suitable value) and 1 (most suitable value). Equal intervals (0-<0.25; >0.25–0.5; >0.5–0.75; >0.75–1) have been generated, which permit comparisons between the different result maps. A description of each indicator and it's calculation in ArcGIS will be presented in the following.

3.3.1. Cold air production

Land Surface Temperature (LST): By retrieving LST, differences between land covers can be detected in order to highlight particularly cool agricultural areas in the MCDA. With the use of Landsat 8 OLI TIR (band 10), land surface temperatures have been derived. After image calibration for band 10, at-satellite brightness temperature (T$_B$) in °C can be calculated by subtracting absolute zero (-273,15 °C) (USGS, 2016):

$$T_B = \frac{K_2}{\ln\left(\frac{K_1}{L_\lambda} + 1\right)} - 273.15 \qquad (4)$$

K_1 (774.8853) and K_2 (1321.0789) are channel-specific coefficients for the thermal transformation, which can be obtained from the supplied Landsat 8 metadata. L_λ is at-sensor spectral radiance of band λ. T_B represents a theoretical value of an ideal black body, so realistic adjustments are further on necessary. Therefore, the spectral emissivity (ε) is required for each object. ε differs depending on the surface condition and can either be derived from existing literature, or calculated in terms of an image-specific average value:

$$\varepsilon = \varepsilon_v * P_v + \varepsilon_s * (1 - P_v) + C \qquad (5)$$

whereby ε_v is the in situ emissivity of vegetation, ε_s is the emissivity of bare soils and *C* represents the surface roughness (Sobrino et al., 2004). The value for ε_v corresponds to 0.973 and for ε_s 0.966 when using Band 10 of a Landsat 8 scene (Wang et al., 2015). *C*= 0, if the surface is smooth and homogeneous. Here, a constant value of 0.005 is used for *C*. The ratio between vegetation and bare soils P_v can be calculated with the *NDVI* as follows:

Table 2
Suitability scores for all six indicators.

Criterion	Indicator	Suitability score (standardized)			
		1 (highly suitable for protection)	0.75 (rather suitable for protection)	0.25 (marginally suitable for protection)	0 (not suitable for protection)
Cold air production	LST [°C]	<25	25–30	>30–35	>35
	Dis2B [m]	0–500	>500–1000	>1000–1500	>1500
	PX [no dimension]	>118.1	>23.1–118.1	>2,4–23.1	0–2.4
Flood retention	Dis2Riv [m]	>50–150	>150–200	>200	0–50
	MASL [m]	<0.5	>0.5–1.5	>1.5–2	>2
Preserve green belts	Dis2Veg [m]	0–250	>250–500	>500–750	>750

Table 3
1 to 9 scale for pairwise comparison matrix (Saaty, 1994).

Intensity of Importance	Definition
1	Equal importance
3	Moderate importance
5	Strong importance
7	Very strong importance
9	Extreme importance
2,4,6,8	Intermediate importance

$$P_v = \left(\frac{NDVI - NDVI_{MIN}}{NDVI_{MAX} - NDVI_{MIN}} \right)^2 \tag{6}$$

$NDVI_{MIN}$ represents the bare soil threshold and $NDVI_{MAX}$ the green vegetation threshold. Typically, a value of 0.2 is to be set for $NDVI_{MIN}$ and 0.5 for $NDVI_{MAX}$ (Avdan and Jovanovska, 2016). The last step is the calculation of LST represented by T_s according to Boltzmann's law based on ε and T_B:

$$T_s = \frac{1}{\varepsilon^{1/4}} * T_B \tag{7}$$

The calculated values were finally reclassified into suitability scores according to human perception of hot and cold temperatures on a summer day in Japan. The same thresholds have also been used for HCMC in a previous study (Doan et al., 2016).

Distance to built up areas (Dis2B): If agricultural and green areas are adjacent to built up areas, it can have a positive effect on health of local residents because of their cold air production and psychological value (Waffle et al., 2017). In particularly urbanized areas, a distance of 1 km to agriculture is appropriate (Maas et al., 2006). Since HCMC is a prospective megacity with a high population density, a threshold distance of 1km was also set for this study. Built up areas of the land cover classification map 2017 were extracted as vector data in ArcGIS and Euclidean distance was calculated for each cell in the study area. The reason why not only settlement but all built up areas were included is that human also spend time at working places, cultural places, schools etc.

Proximity Index (PX): The size and geometric structure of open spaces are of crucial importance for the amount of cold air production (Eckert, 2013; Syrbe et al., 2017). In this sense, small and isolated agricultural areas are less worthy of protection than large, contiguous areas. However, small but networked agricultural areas also ensure cold air production (Storch et al., 2012). According to Gustafson and Parker, the Proximity Index (PX) acts as an adequate measuring instrument, as it considers both the size and the networking of individual patches within a landscape (Gustafson and Parker, 1994). Therefore, the freely available landscape analysis program FRAGSTATS 4.27 was used (McGarigal, 2015).

$$PX = \sum_{i=1}^{n} \left(\frac{S_i}{Z_i} \right) \tag{8}$$

For each patch, a value is calculated on a grid basis, whereby PX

equals the division of the sum of a patch area S_i [m^2] and the squared distance Z_i [m^2] to the neighbor patches of the same type located in a certain search radius (see ibid.). The measurement takes place between the cell centers. For the raster grid calculation, rice paddies, annual plants, and perennial plants of the land cover map 2017 were grouped to a single agriculture class and transformed into ASCII-format for calculation in FRAGSTATS 4.27. Due to the Landsat grid cell size of 30m, a search radius of 100m was set to include the probability of other land covers between agricultural patches. PX scores high values when a patch is surrounded by large or continuous patches (connectivity) and small values when it is fragmented (isolation). Because the calculated values differ from city to city, no scientific thresholds for suitability evaluation exist. For this reason, four equal quantiles were defined and standardized.

3.3.2. Flood retention

Distance to Rivers (Dis2Riv): With increasing distance to running waters, discharge conditions are no longer optimally met. For this reason, agricultural land should be preserved, if it is located near rivers. At the same time, agricultural land shouldn't be located directly along rivers, since here crop plants can wash away due to excessive water erosion. Storch et al. propose a three-level division into so-called "taboo zones", "buffer zones" and "flood-safe zones" for the area around rivers (Storch et al., 2012). The taboo zone is particularly prone to flooding, which means that no anthropogenic uses, but tree plantings to erosion resistance should exist. The buffer zone represents the area in which flooding is possible but can be compensated by the specific drainage functions of certain land uses. Here, agricultural areas and public parks represent the dominant land use. At the higher lying flood-safe zone, the localization of settlement areas and other public facilities begins.

For the MCDA, rivers and channels were selected and extracted from the land use map of 2010. This was followed by manual adjusting of the data set on the basis of the SPOT 5 imagery in order to ensure the most up-to-date distribution of the river-network in HCMC. By doing so, this process excludes artificial aquaculture ponds. The average airline distance from built up areas to rivers and canals in ArcGIS was calculated (200m) to create a threshold for the flood-safe zone. The space between rivers and built up areas was divided into 50m intervals based on the Euclidean distance and assigned to the standardized suitability values in raster grid calculation.

Meters above sea level (MASL): The MASL indicator serves as a complement to the Dis2Riv indicator in order to take geomorphological factors into account. Low-lying agricultural areas provide a catch for down-flowing river water and thus can reduce flood risks in settlement areas or vulnerable infrastructures (Downes and Storch, 2014). At a height of 1.5m–2m above sea level, the flooding hazard of settlement areas in HCMC is steadily decreasing, so agricultural land no longer serves its catching function (Phoung Chau, 2013). With this in mind, the provided DEM was reclassified into a new range of suitability scores for MCDA.

Table 4
Final indicator weightings of pairwise comparison.

Indicator	LST	Dis2B	PX	Dis2Riv	MASL	Dis2Veg	Weighting	Rank
LST	1	1/2	1/8	1/7	1/4	1/7	0.03	6
Dis2B	2	1	1/7	1/5	1/6	1/5	0.04	5
PX	8	7	1	3	7	2	0.4	1
Dis2Riv	7	5	1/3	1	4	1/3	0.18	3
MASL	4	6	1/7	1/4	1	1/5	0.1	4
Dis2Veg	7	5	1/2	2	5	1	0.25	2
CR = 0,08							$\sum = 1$	

3.3.3. Preservation of green belts

Distance to Vegetation (Dis2Veg): An adjacent arrangement of agricultural and natural areas may lead to cooperative effects such as particulate matter filtration or the extension of habitat for edge-sensitive animals. Furthermore, agriculture serves as an upstream use in the sense of a green belt around the city's urban core and is therefore to be maintained where it is located adjacent to vegetation and forests. For the MCDA, the classes *forests* land and *lower vegetation* of the land cover classification map 2017 were extracted and grouped. After that, equal intervals were formed by Euclidean distance buffers from vegetation borders.

Table 2 shows the final classification of each indicator corresponding to its standardized suitability score by reclassifying raster cells in ArcGIS with the Spatial Analyst Tool.
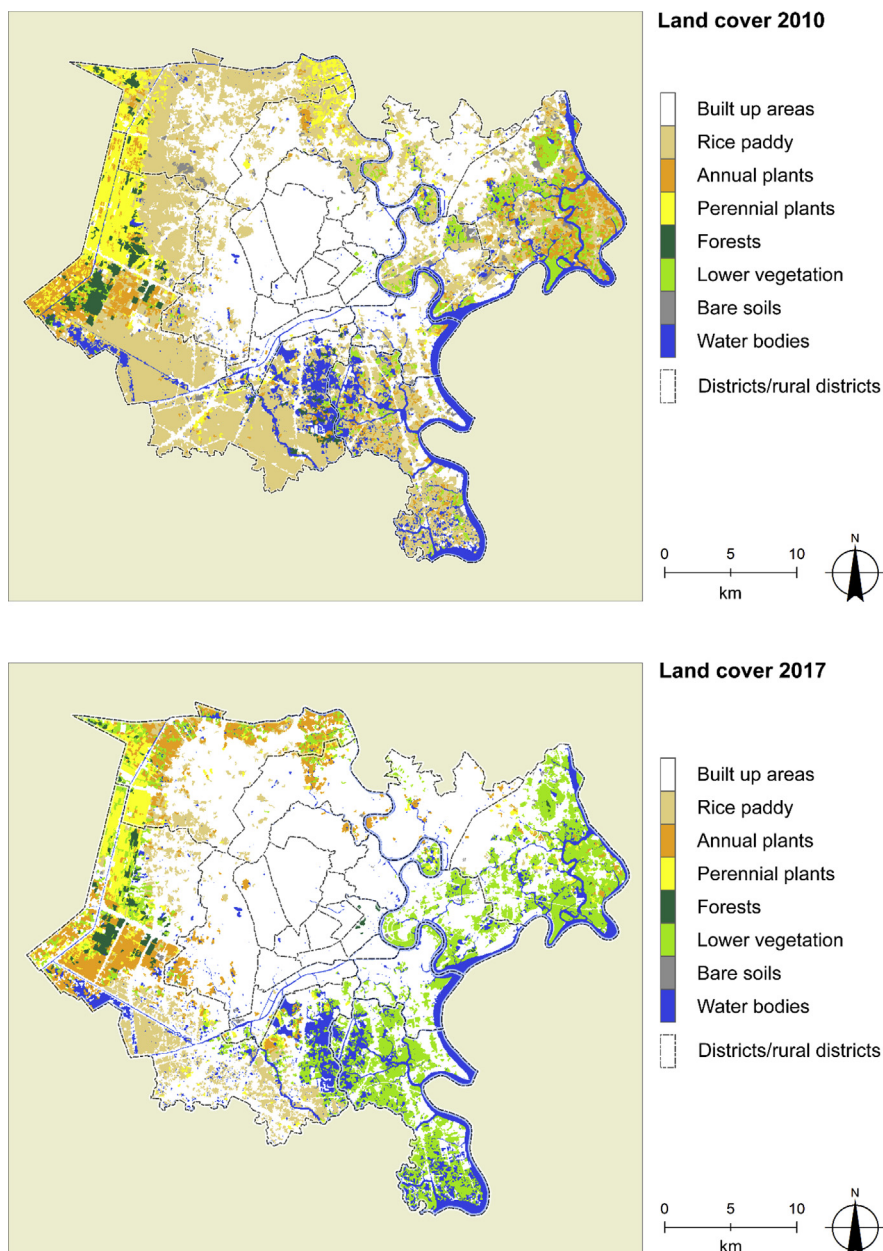

Fig. 2. Land cover classification results for the study area.

Table 5

Accuracy assessment statistics of land cover classification [%].

year	Land cover class	Built up areas	Rice paddy	Annual plants	Perennial plants	Forests	Lower Vegetation	Bare soils	Water bodies	O_A	k
2010	U_A	85.71	77.78	84	66.67	90.48	91.67	95.83	100	85.57	0.83
	P_A	92.31	80.77	80.77	84.62	73.08	84.62	88.46	100		
2017	U_A	70.27	92.59	80.77	100	100	73.08	100	92.86	87.01	0.85
	P_A	100	96.15	80.77	73.08	100	73.08	73.08	100		

Table 6

Land cover data of the classification results.

Land cover	2010		2017		change	
	[km²]	[%]	[km²]	[%]	[km²]	[%]
Built up areas	378.4	39.6	568.5	59.4	+190.1	+50.2
Rice paddy	310.2	32.4	51.0	5.3	-259.2	-83.5
Annual plants	50.8	5.3	54.3	5.7	+3.6	+6.8
Perennial plants	55.6	5.8	32.3	3.4	-23.3	-41.1
Forests	16.5	1.7	9.6	1.0	-6.8	-41.8
Lower vegetation	36.0	3.8	133.2	13.9	+97.2	+270
Bare soils	9.8	1.0	1.6	0.2	-8.2	-83.7
Water bodies	99.4	10.4	106.0	11.1	+6.6	+6.6
$\sum$	956.6	100.0	956.6	100.0	-	-

3.4. Defining weighting factors

With the use of AHP, relative weights for each indicator were calculated, because their degree of importance in the suitability analysis may differ. Two experts of agricultural and environmental planning were interviewed for the final indicator weightings, as they tend to have greater experience about the phenomenon. By doing so, the quality of the suitability analysis can be improved by enhancing transparency.

The core procedure of the AHP lies in a pairwise comparison of two indicators each (Brunelli, 2015). For the pairwise comparison A-matrix, Saaty's 1 to 9 scale (Table 3) was used, which represents a numerical weight ratio to assess the relevance of an indicator to the protection potential. After the pairwise comparison, the column sums of the A-matrix were first calculated. This is followed by a normalization of the A-matrix, resulting in a B-matrix. Via the B-matrix values, the relative indicator weighting were calculated by averaging. As a result, each indicator is ranked by importance. The total of all relative weights will be always 1 (according to 100%).

In order to check the consistency of the experts' judgements in pairwise comparison, the determination of a consistency ratio (CR) is implemented in the AHP. For this purpose, Aw_i was first calculated by multiplying the A-matrix by the relative weightings w_i. This was followed by the calculation of the eigenvalues λ_i:

$$\lambda_i = \frac{Aw_i}{w_i} \quad (i = 1\ (1)\ n) \tag{9}$$

The consistency index (CI) can be determined using the average of all eigenvalues λ_{max} and the specific number of indicators n considered:

$$CI = \frac{\lambda_{max} - n}{n - 1} \tag{10}$$

The ratio of CI and the random index (RI) reveals CR:

$$CR = \frac{CI}{RI} \tag{11}$$

RI is tabularly provided by Saaty. Depending on the number of indicators, a different value has to be selected. In our case -respecting a total of six indicators-, a value of 1.25 has to be taken (Saaty, 1994). With CR= 0.08, the consistency requirements (CR < 0.1) according to Saaty are satisfied (Thinh and Vogel, 2007). The expert on agriculture chose the most important factor for PX, while the expert for environmental planning assigned Dis2Veg the most importance. The final indicator weightings are listed in Table 4. Compared with the other indicators, PX has the highest weighting of 40%, because if an agricultural area is too small and isolated, it has no benefit in terms of cold air production or flood retention. On the other hand, LST is of minor relevance to the protection suitability, as the indicator only contributes to a positive effect when the agricultural area is close to built up areas. For this reason, Dis2B is weighted higher than LST.

Fig. 3. Abandoned agricultural land in the southern rural district Nhà Bè.

Table 7

Land cover transition matrix for 2010–2017.

		2010							
Land cover [km²]		Built up areas	Rice paddy	Annual plants	Perennial plants	Forests	Lower vegetation	Bare soils	Water bodies
2017	Built up areas	363.2	150.2	11.2	17.2	1.6	8.5	6.0	10.6
	Rice paddy	1.3	45.8	0.8	0.7	0.4	0.0	1.5	0.5
	Annual plants	1.9	27.6	11.2	7.3	3.1	1.6	0.2	1.4
	Perennial plants	0.6	7.3	4.9	15.7	2.7	0.6	0.2	0.2
	Forests	0.3	0.8	0.6	2.6	4.5	0.9	0.0	0.1
	Lower vegetation	6.6	60.1	19.2	11.3	3.5	22.5	1.7	8.3
	Bare soils	0.2	0.7	0.2	0.1	0.1	0.2	0.1	0.0
	Water bodies	4.2	17.6	2.8	0.8	0.6	1.7	0.1	78.3

3.5. Multi-Criteria-Decision-Analysis

Once the indicator grids and their relative weights are obtained, the CP procedure can be applied on each raster layer to produce the result maps of agricultural areas suitable for protection. Referring to the CP equation, all suitability scores of each individually weighted indicator are aggregated:

$$L_p\left(W\right) = \left[\sum_{j=0}^{n} W_j^p \left|\frac{Z_j^* - Z_j(x)}{Z_j^* - Z_{*j}}\right|^p\right]^{1/p} \rightarrow min \qquad (12)$$

W_j represents the individual weight of each alternative with respect to the suitability of protection, taking into account that $W_j > 0$, $W_1 + W_2 + .. + W_n = 1$. $L_p(W)$ is the weighted distance of each alternative to the ideal point Z_j^*. The opposite of Z_j^* is Z_{*j}, which describes the worst value an alternative can assume. The more $L_p(W)$ reaches towards 0 ($\rightarrow min$), the closer the element to the protection potential and vice versa. p can assume natural values of ≥ 1 and is used to weight the discrepancy between the ideal point and the actual measured value of an indicator $Z_j(x)$. With this in mind, the added power reflects the degree of compensation. If $p = 1$, a City-Block-Norm is given, in which poorly rated alternatives can be compensated by well rated alternatives. The opposite is the Maximum-Norm with $p = \infty$. In case of $1 < p < \infty$ (Euclidean-Norm), partial compensation applies. Consequently, the parameters W_j and p are directly influencing the compromise solution.

4. Results and discussion

4.1. Classification results and change detection

The results of the land cover classification are illustrated in Fig. 2, with $O_A = 85{,}57\%$ and $k = 0{,}83$ for Landsat 2010 and $O_A = 87{,}01\%$ and $k = 0{,}85$ for Landsat 2017. For both 2010 and 2017, the overall accuracy is above the 85% limit according to Anderson et al., so the results are initially considered acceptable for post-classification comparison (Anderson et al., 1976). The accuracy increased for 2017 because of a higher spectral resolution of Landsat 8 and the availability of more detailed reference material like field observations (Table 5).

Firstly, for every land cover class a visual change in its spatial distribution becomes noticeable. New urbanization processes can be detected in almost every direction, whereby existing roads often provide the place of origin, which is particularly evident in the west. Given these points, the built up area has increased by 190.1 km² within seven years, accounting for 59.4% of the total area in 2017 (Table 6). These findings imply that the existing urbanization problem not only lies in the absolute land consumption, but also in its distribution.

In contrast, a tremendous decrease of rice paddy in the north, the west and the south took place. While the study area has been surrounded by 32,4% of rice paddy in 2010, in 2017 only 5,3% is covered by that land cover (Table 6). On the one hand, this fact can be explained by the parallel urban expansion. On the other hand, e.g. in the rural district Hóc Môn, rice cultivation gets increasingly substituted by vegetable cultivation, as the south-adjacent Mekong Delta represents a strong competitor in rice production (Vu and Kawashima, 2017). Under those
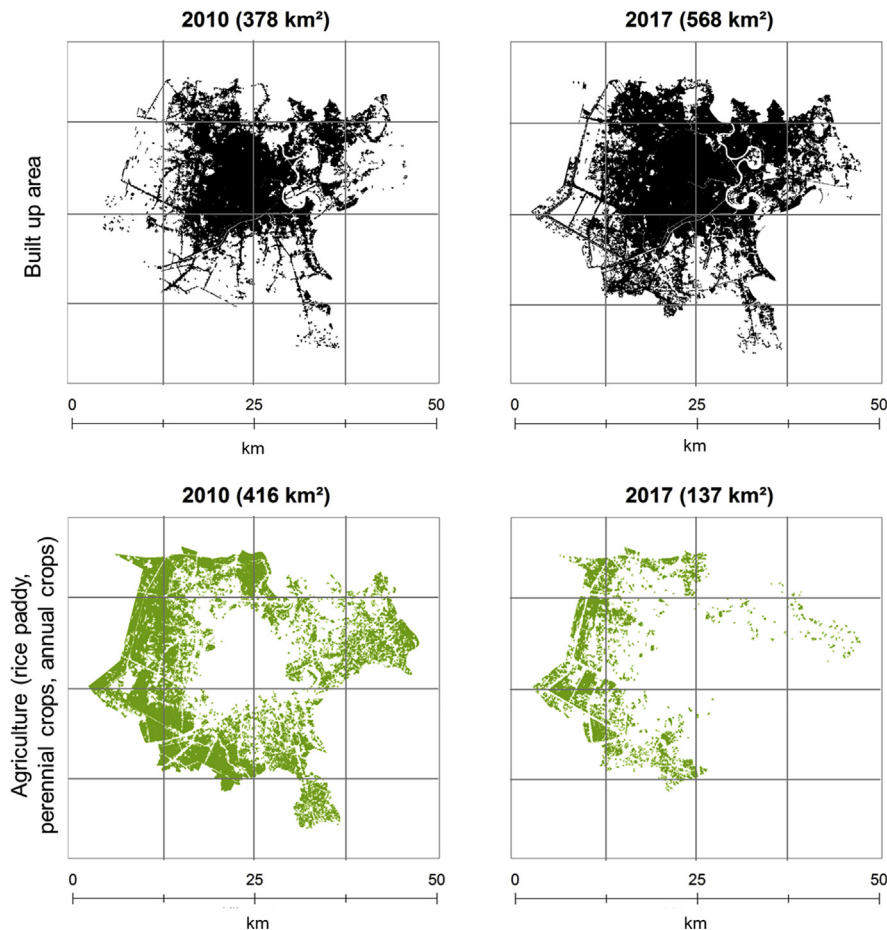

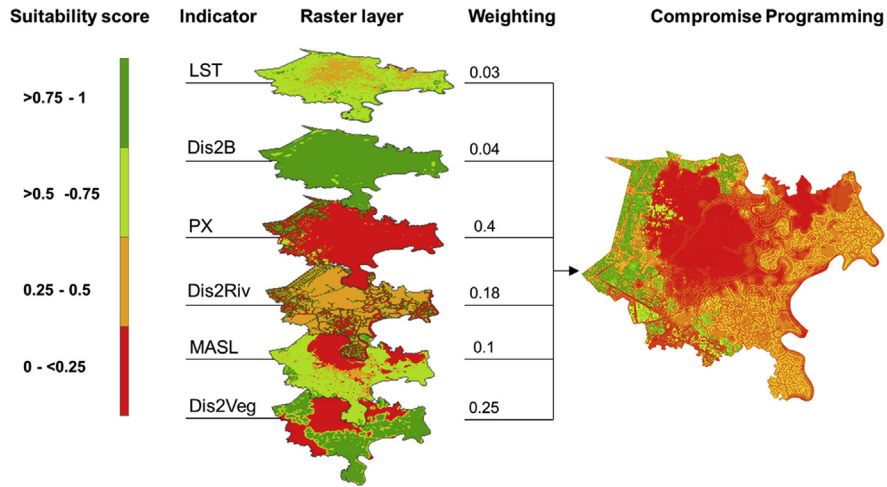**Fig. 4.** Structural changes in the study area regarding agriculture and built up area.

Fig. 5. Schematic procedure of the GIS-based CP method.

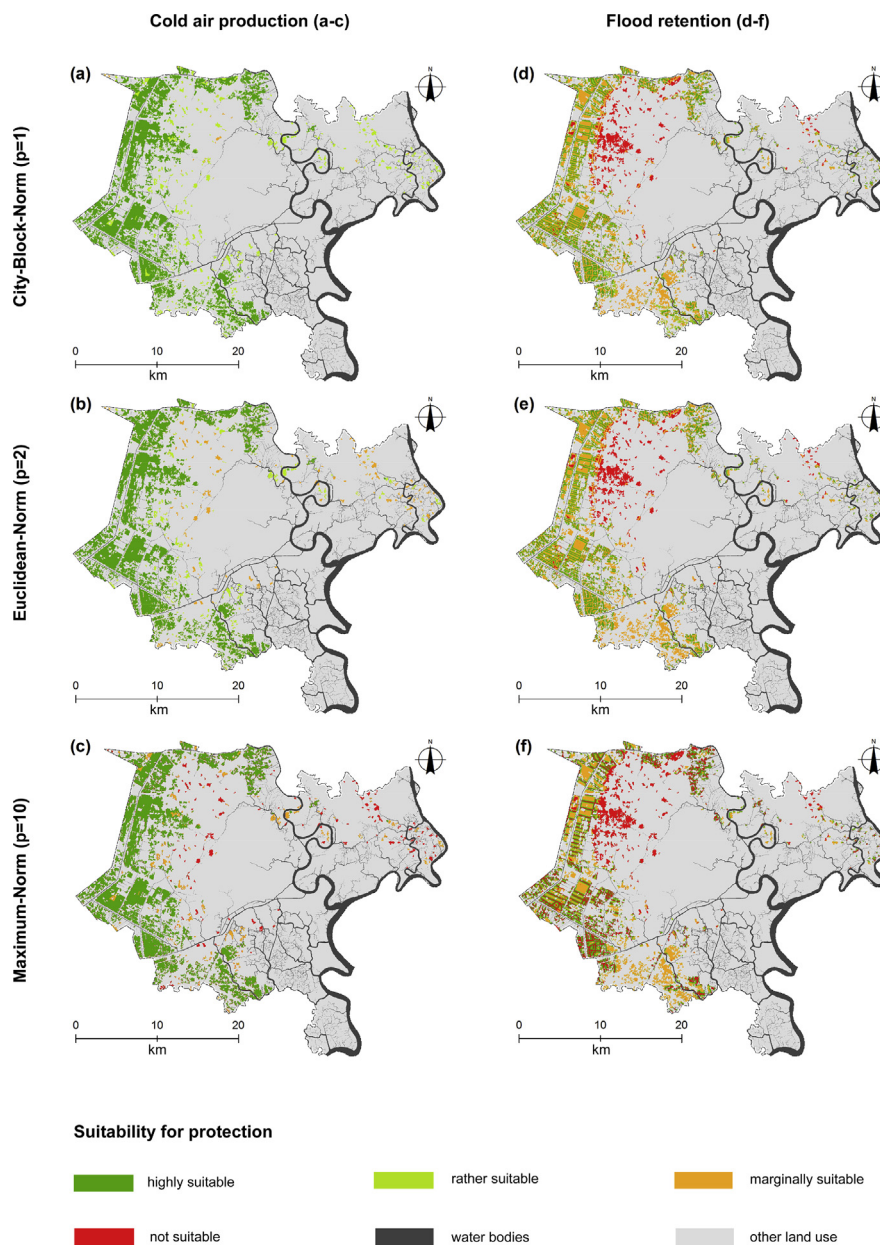**Fig. 6.** Results of the partial evaluations for the two criteria *Cold air production* (a–c) and *Flood retention* (d–f) using three scenarios.

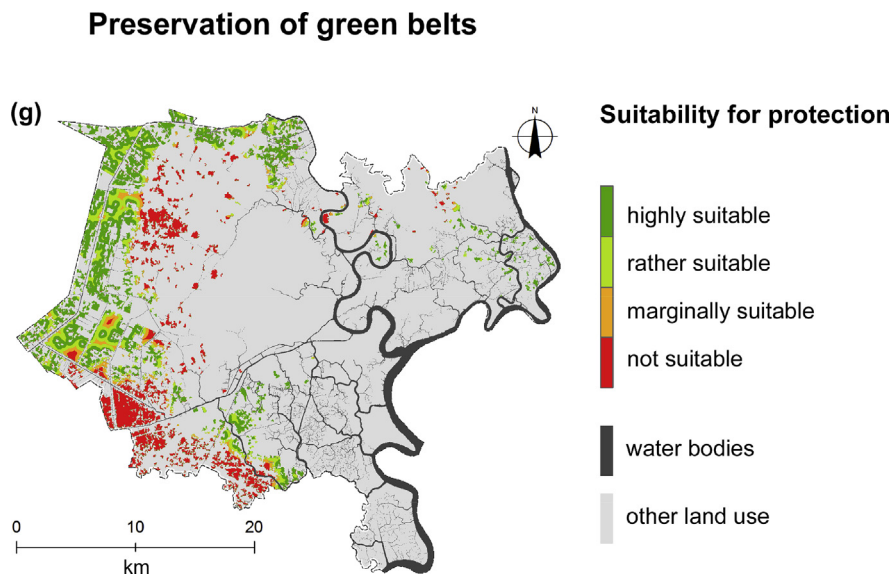## Preservation of green belts

Fig. 7. Results of the partial evaluation for the criteria *Preservation of green belts*.

circumstances, the increase of annual plants in Hóc Môn is reasonable. In the end, most of the leftover paddy rice fields are located in the south-western part of the city, blending seamlessly with the rice fields of the Mekong Delta.

However, this competitive relationship also forces many farmers in HCMC to completely abandon rice production, which ends up in fallow fields and uncontrolled natural vegetation development represented by lower vegetation. In the rural district Nhà Bè in particular, this phe-nomenon can be confirmed by the land cover classification for 2017 and the authors' ground observations (Fig. 3).

Nonetheless, the remarkable increase of lower vegetation (+270%) could also represent new pastures. Again, pastures as a single land cover class cannot be taken into account in our study, as they do not visually differ from lower vegetation. Based on this, the growing economy and the increasing consumption of meat in HCMC speak in favor of a trend to-wards cattle breeding. For example, between 2011 and 2015, the total number of cattle in HCMC increased by 30.000. Simultaneous, the poultry stock grew by more than 500.000 units (Statistical Office HCMC, 2015b).

Also, the share of perennial crops in Quận 12 has noticeably decreased by 41.2% during the investigation period. The reduction of bare soils could result from the mentioned fact that several large-scale projects for new housing were in the implementation in the south and east by the year 2010, which entailed a corresponding number of con-struction sites, including sand spills.

As previously noted, shrimp and fish farming have become more important in HCMC and surrounding regions for several years. Therefore, the increase of water bodies by 6.6km^2 is logical. Most aquacultures are located in the southern rural districts Nhà Bè and Bình Chánh.

With a land cover transition matrix, transformations of individual land cover classes can be quantified from an initial state to a final state, so the actual type of change becomes more obvious (Table 7). For each initial land cover class, the matrix indicates how these pixels were reclassified to the final state. Accordingly, each column sum is the starting area of a class for the year 2010 and each row sum is the resulting area for the year 2017. Diagonal entries illustrate all pixels that remained in their initial state. Accordingly, each column summation is the area of a class by the year 2010 and each row summation is the area by the year 2017. For example, 150.2 km^2 of rice paddy was classified as built up area in 2017.

The developments described previously can be confirmed here once again: A large part of the observed loss of rice paddy is due to urban

expansion. In some cases, however, rice paddy areas were also converted to annual crops or even abandoned and therefore developed into new grassland. That situation is similar for other crops, but to a lesser extent. As a result, in 2017 an east-west disparity in the spatial distribution of agricultural land can be observed (Fig. 4).

4.2. Evaluation of agricultural protection sites

In order to test the method and to illustrate the different effects of the compensation measures, three scenarios were performed with $p=1$, $p=2$ and $p=10$ respectively $p=\infty$. Fig. 5 illustrates the schematic procedure in ArcGIS. The result is a raster-based weighted summation of the six singular indicators with standardized values ranging between 0 and 1. The higher the suitability value, the closer the alternative and its attri-butes are to the ideal point.

4.2.1. Partial evaluation

In the context of CP method, it is possible to calculate partial suit-ability maps for the three criteria of *Cold air production, Flood retention* and *Preservation of green belts*. In this case, all indicators are weighted equally because they do not refer to the main objective, but to one of the three subordinate criteria. Again, with the exception of the indicator Dis2Veg, three compensation scenarios were carried out with $p=1$, $p=2$ and $p=10$. Since Dis2Veg is the only indicator representing the criterion *Preservation of green belts*, there is no need for compensation between the alternatives. Fig. 6 and Fig. 7 show the result maps of the partial evalu-ations including the existing agricultural areas of the land cover classi-fication results (137 km^2) in 2017.

For the criterion *Cold air production*, the first three indicator grids for LST, Dis2B and PX were aggregated according to the CP equation in ArcGIS (Fig. 6 a-c). The option of p creates a range for the ultimate assessment of the need for protection. This is also apparent considering the decreasing average suitability score for the raster cells from 0.84 (a) to 0.67 (c). In the case of the City-Block-Norm, almost all areas are above the 0.5 limit (rather suitable for protection). With the Maximum-Norm, all small, isolated areas are rated worst. Because these raster cells do not offer the maximum target performance of PX, they are completely eliminated in that case. This effect can be observed in the east and parts of the west. Similarly, large and contiguous areas in the districts of Bình Chánh and Hóc Môn reach higher values and represent suitable cold air production sites near built up areas.

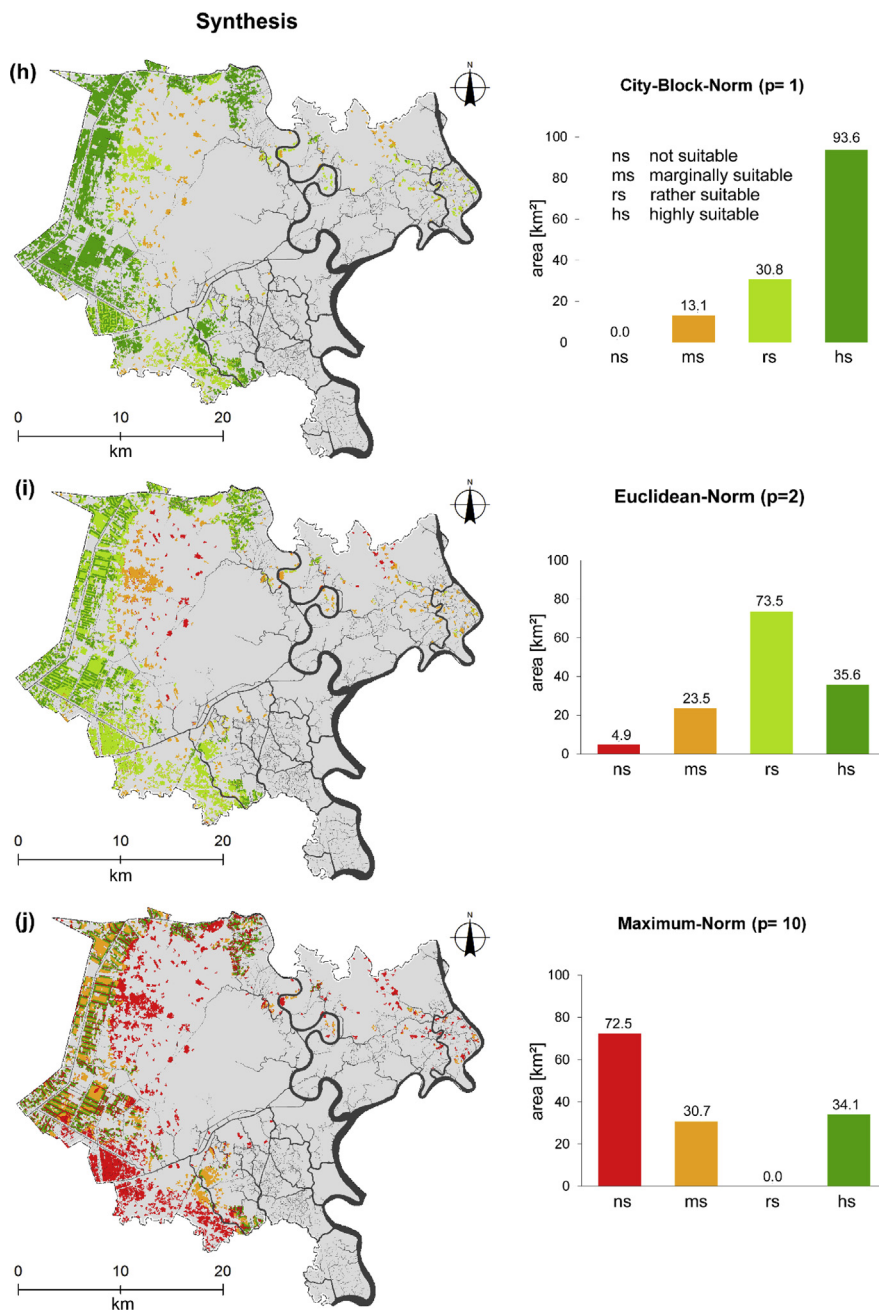Fig. 6 (d-f) illustrates the assessment of the criterion *Flood retention*

Synthesis

Fig. 8. Final results of the synthesis (*Cold air production*, *Flood retention* and *Preservation of green belts*) using three scenarios.

based on the aggregation of the two indicator grids Dis2Riv and AMSL. Higher values are representing low-lying, river-related agricultural areas. High-lying raster cells in the northwest are rated worse. The average suitability value for protection diminishes with reduced compensation and reaches its minimum at 0.40 (f). In comparison to the criterion *Cold air production*, fewer agricultural areas are suitable for protection here.

Preservation of green belts is the last of the three partial evaluations, where the single indicator Dis2Veg is used for quantification. Fig. 7 (g) illustrates that there is a high potential for protection in the west due to the proximity to forest areas. In the southern district of Nhà Bè, there are also some natural connections. However, a large area between the districts of Bình Chánh and Hóc Môn has few values suitable for protection because it is not surrounded by natural vegetation but forms a mixture of settlement area and agriculture. The choice of the Euclidean distance to forests and lower vegetation as a quantitative measurement is thus problematic in two ways: Firstly, the clear limits prevent a transition to

more remote agricultural areas. On the other hand, this research does not take into account natural areas located outside of the study area. This is why rice paddies in the southwest do not show any networking tendencies to the adjacent fields of the Mekong Delta

4.2.2. Synthesis

The synthesis was carried out to generate a final result grid, taking into account every individual indicator weight obtained with the AHP method. This means, that grid cells with a high suitability value do justice to both the *Cold air production*, *Flood retention* and the *Preservation of green belts* (Fig. 8).

Higher rated raster cells are located in the north of Hóc Môn and to a large extent in Bình Chánh along the densely populated urban core. The competitive relationship between the six indicators becomes particularly clear in the case of the Maximum-Norm. Although PX with the highest weighting of 0.4 should have a noticeable effect on the result, any suit-
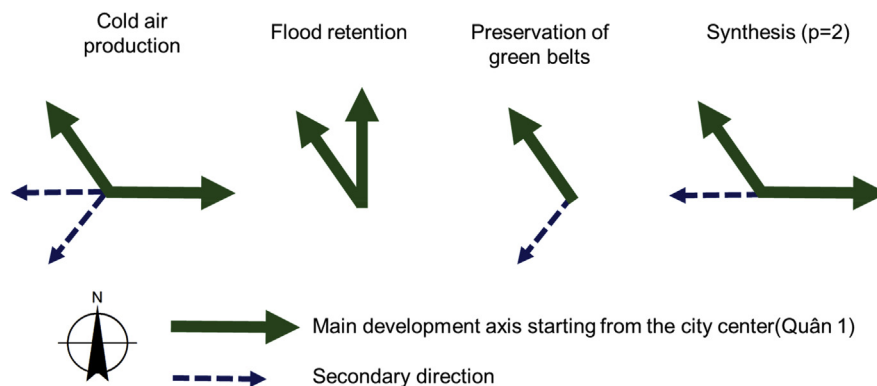
Fig. 9. Possible urban development direction depending on partial evaluation and synthesis. (Source: modified version of Du, 2015).

ability for protection does not apply unless all indicators match the ideal point. Also, the strict thresholds between the suitability scores emerge by less compensation. For this reason, if $p = 10$, only linearly arranged grid cells of high suitability scores remain along streams and rivers (j). In total, between the scenarios $p = 2$ and $p = 10$ there are 73.5km^2 of agricultural area rather suitable for protection, but the reduction of agricultural land highly suitable for protection is marginal in this respect. Given these points, it is questionable to define policy implications according to both the Maximum- and City-Block-Norm. With the Euclidean-Norm, a compromise solution can be created, which will be discussed in the following.

4.3. Policy implications

Both the MCDA and the land cover change detection clearly show that regulation of urban expansion is required and that agricultural land in combination with natural vegetation should be respected equally in future planning decisions. One premise here is to promote urban development in such areas that create unsuitable site conditions for agricultural protection and vice versa. Initially, it is possible to subdivide specific protection guidelines into subprojects and implement them gradually in accordance with the three criteria of *Cold air production*, *Flood retention* and *Preservation of green belts*. Fig. 9 can be interpreted as a potential solution on the current dilemma of land use planning in HCMC discussed in chapter 2. Depending on the partial evaluations, different main urban development axes can be defined which leave protected agricultural areas unaffected.

If the realization of main development axes is not feasible, secondary axes represent possible bypass directions. According to Fig. 9, the dominant development directions should be the east and northwest. The fact that isolated, higher-lying agricultural areas in Quận 9 and Thủ Đức are not considered to be worth protecting supports the idea of an eastward urban development. This option is reinforced by the fact that the project Thủ Thiêm in Quận 2 should serve as a new CBD in the future, thus shifting important utilities further east. Adhering to a maximum annual net consumption of agricultural land per district, rational urban expansion with agricultural and green areas between the development corridors is thus possible. Even in the case of sealing agricultural land not suitable for protection, the concept of avoidance should nevertheless exist. This may include the establishment of an eco-account and the obligation to compensate lost agriculture in- or ex-situ. In the case of ex-situ compensation, new agricultural land could be located near rivers, adjacent to consisting agricultural land or even on rooftops. A dialogue between agriculture and settlements like urban agriculture is also conceivable (Giseke et al., 2015).

It must be mentioned that agricultural land can also have negative external effects that contribute to climate change and environmental damage (greenhouse gases, soil degradation through over-fertilization, pollutants entering water bodies etc.) (see Turner et al., 1995: 39).

Nevertheless, a strict regulation with emission limit values and the issuing of certificates for a sustainable symbiosis between agriculture, nature and settlements is necessary.

5. Conclusion

Our presented study is the first demonstration of established GIS- and remote-sensing-based techniques for evaluating the suitability for protection of agricultural land in HCMC. Based on a small, up-to-date and almost freely available dataset, meaningful policy guidance to planners on a regional scale could be achieved. Both disciplines can also be applied for other megacities as a useful and interdisciplinary tool for local planning authorities and scientists. Especially for spatial and environmental planning, the results are of particular interest, because agriculture has long ceased to be reduced to a producer, but also fulfills important services in case of climate adaptation and environmental protection.

However, there also exist several limitations to the study. The fact, that a pixel-based classification only allows to map land *covers* inhibits explanatory power to the massive increase of lower vegetation during the research period. The suspicion of an agricultural trend towards cattle breeding couldn't be adequately solved in our study framework and will require further investigation. One approach should be multi seasonal imagery classification for both dates, in order to consider different phenological stages of vegetation cover. Further expert and stakeholder knowledge is conducive to cover as many disciplines as possible in order to optimize decision making and indicator weightings. Of course, Landsat-based image classification does not allow highly detailed statements about land cover change, but it provides an acceptable basis for initial assessment of structural trends. Nevertheless, the accuracy of the findings should be increased with further ground observations or satellite data with finer spatial resolution. For this study, the indicated land cover changes are important to localize remaining agricultural areas and to assess future urban settlement directions regarding sustainable urban development. In the long run, finding a balance between economic growth, climate adaptation and environmental protection should be of primary importance for HCMC.

Declarations

Foundation (TU Dortmund University) and was also supported by Deutsche Forschungsgemeinschaft and TU Dortmund University within the funding programme Open Access Publishing.

Competing interest statement

Additional information

No additional information is available for this paper.

Acknowledgements

References

AbdelRahman, M.A.E., Natarajan, A., Hegde, R., 2016. Assessment of land suitability and capability by integrating remote sensing and GIS for agriculture in Chamarajanagar district, Karnataka, India. Egypt. J. Rem. Sens. Space Sci. 19 (1), 125–141.

Ahmad, A., Quegan, S., 2012. Analysis of maximum likelihood classification on multispectral data. Appl. Math. Sci. 6 (129), 6425–6436.

Anderson, J.R., Hardy, E.E., Roach, J.T., Witmer, R.E., 1976. A Land Use and Land Cover Classification System for Use with Remote Sensor Data. U.S. Geological Survey Professional Paper 964.

Avdan, U., Jovanovska, G., 2016. Algorithm for automated mapping of land surface temperature using LANDSAT 8 satellite data. J. Sens. (2), 1–8.

Baig, M.H.A., Zhang, L., Shuai, T., Tong, Q., 2014. Derivation of a tasselled cap transformation based on Landsat 8 at-satellite reflectance. Rem. Sens. Lett. 5 (5), 423–431.

Brennan, R.L., Prediger, D.J., 1981. Coefficient Kappa: some uses, misuses, and alternatives. Educ. Psychol. Meas. 41 (3), 687–699.

Brunelli, M., 2015. Introduction to the Analytic Hierarchy Process (Eng). Springer International Publishing, Cham s.l., 83 pp.

Congalton, R.G., Green, K., 2009. Assessing the Accuracy of Remotely Sensed Data: Principles and Practices, 2. CRC, Boca Raton Fla u.a., [XV], 183 S.

Crist, E.P., Cicone, R.C., 1984. A physically-based transformation of thematic mapper data-the TM tasseled cap. IEEE Trans. Geosci. Remote Sens. 256–263.

Disperati, L., Virdis, S.G.P., 2015. Assessment of land-use and land-cover changes from 1965 to 2014 in Tam Giang-Cau Hai lagoon, central Vietnam. Appl. Geogr. 58, 48–64.

Doan, Q.-V., Kusaka, H., Ho, Q.-B., 2016. Impact of future urbanization on temperature and thermal comfort index in a developing tropical city: Ho Chi Minh City. Urban Clim. 17, 20–31.

Downes, N.K., Storch, H., 2014. Current constraints and future directions for risk adapted land-use planning practices in the high-density asian setting of Ho Chi Minh city. Plann. Pract. Res. 29 (3), 220–237.

Downes, N.K., Storch, H., Schmidt, M., van Nguyen, T.C., Dinh, L.C., Tran, T.N., Hoa, L.T., 2016. Understanding Ho Chi Minh city's urban structures for urban land-use monitoring and risk-adapted land-use planning. In: Katzschner, A., Waibel, M., Schwede, D., Katzschner, L., Schmidt, M., Storch, H. (Eds.), Sustainable Ho Chi Minh City: Climate Policies for Emerging Mega Cities. Springer International Publishing, Cham, pp. 89–116.

Du, Huynh, 2015. The misuse of urban planning in Ho Chi Minh City. Habitat Int. 48, 11–19.

Dutta, S., Patel, N.K., Medhavy, T.T., Srivastava, S.K., Mishra, N., Singh, K.R.P., 1998. Wheat crop classification using multidate IRS LISS-I data. J Indian Soc Remote Sens 26 (1-2), 7–14.

Eckert, R., 2013. Resilientes Ho Chi Minh City: Das Ende der kompakten südostasiatischen Stadt? In: Waibel, M. (Ed.), Ho Chi Minh MEGA City. Regiospectra-Verl., Berlin, pp. 181–200.

Fitzpatrick-Lins, K., 1981. Comparison of sampling procedures and data analysis for a land-use and land-cover map. Photogramm. Eng. Rem. Sens. 47 (3), 343–351.

Gilmore, S., Saleem, A., Dewan, A., 2015. Effectiveness of DOS (Dark-Object Subtraction) method and water index techniques to map wetlands in a rapidly urbanising megacity with Landsat 8 data. B. Veenendaal and A. Kealy 100–108.

Giri, C.P., 2012. Remote Sensing of Land Use and Land Cover: Principles and Applications (Eng). CRC Press, Hoboken, p. 469.

Giseke, U., Gerster-Bentaya, M., Helten, F., Kraume, M., Scherer, D., Spars, G., Amraoui, F., Adidi, A., Berdouz, S., Chlaida, M., Mansour, M., Mdafai, M. (Eds.), 2015. Urban Agriculture for Growing City Regions: Connecting Urban-Rural Spheres in Casablanca (Eng). Routledge/Earthscan, London, New York, p. 567.

Goldblatt, R., Deininger, K., Hanson, G., 2018. Utilizing publicly available satellite data for urban research: mapping built-up land cover and land use in Ho Chi Minh City, Vietnam. Dev. Eng. 3, 83–99.

Gravert, A., Wiechmann, T., 2016. Climate change adaptation governance in the Ho Chi Minh city region. 19-33. In: Katzschner, A., Waibel, M., Schwede, D., Katzschner, L., Schmidt, M., Storch, H. (Eds.), Sustainable Ho Chi Minh City: Climate Policies for Emerging Mega Cities. Springer International Publishing, Cham.

Gustafson, E.J., Parker, G.R., 1994. Using an index of habitat patch proximity for landscape design. Landsc. Urban Plan. (29), 117–130.

HARMS, E., 2013. Eviction time in the new saigon: temporalities of displacement in the rubble of development. Cult. Anthropol. 28 (2), 344–368.

Hirsch, P., 2017. Routledge Handbook of the Environment in Southeast Asia, 1. Routledge, London, New York online resource (xviii, 521).

Katzschner, L., Burghardt, R., 2013. Bedeutung des Stadtklimas für eine nachhaltige Entwicklung von Ho Chi Minh City. In: Waibel, M. (Ed.), Ho Chi Minh MEGA City. Regiospectra-Verl., Berlin, pp. 259–268.

Kauth, R.J., Thomas, G.S., 1976. The Tasselled Cap – A Graphic Description of the Spectral-Temporal Development of Agricultural Crops as Seen by LANDSAT. LARS Symposia. Paper 159.

Kihoro, J., Bosco, N.J., Murage, H., 2013. Suitability analysis for rice growing sites using a multicriteria evaluation and GIS approach in great Mwea region, Kenya (eng). SpringerPlus 2 (1), 265.

Kontgis, C., Schneider, A., Fox, J., Saksena, S., Spencer, J.H., Castrence, M., 2014. Monitoring peri-urbanization in the greater Ho Chi Minh City metropolitan area. Appl. Geogr. 53, 377–388.

La Rosa, D., Barbarossa, L., Privitera, R., Martinico, F., 2014. Agriculture and the city: a method for sustainable planning of new forms of agriculture in urban contexts. Land Use Policy 41, 290–303.

Laux, P., Nguyen, P.N.B., Cullmann, J., Kunstmann, H., 2017. Impacts of land-use/land-cover change and climate change on the regional climate in the central Vietnam. In: Nauditt, A., Ribbe, L. (Eds.), Land Use and Climate Change Interactions in Central Vietnam: LUCCi, , first ed.30. Springer, Singapore, pp. 143–151.

Li, X., Yeh, A.G.-O., 2001. Zoning land for agricultural protection by the integration of remote sensing, GIS, and cellular automata. Photogramm. Eng. Rem. Sens. (67), 471–477.

Maas, J., Verheij, R.A., Groenewegen, P.P., de Vries, S., Spreeuwenberg, P., 2006. Green space, urbanity, and health: how strong is the relation? (eng). J. Epidemiol. Community Health 60 (7), 587–592.

Malczewski, J., 2004. GIS-based land-use suitability analysis: a critical overview. Prog. Plann. 62 (1), 3–65.

Maplecroft, 2012. Climate Change Vulnerability Index 2013 – Most at Risk Cities accessed. https://www.preventionweb.net/files/29649_maplecroftccvisubnation almap.pdf. (Accessed 21 August 2018).

Marinoni, O., 2004. Implementation of the analytical hierarchy process with VBA in ArcGIS. Comput. Geosci. 30 (6), 637–646.

McCoy, R.M., 2005. Field Methods in Remote Sensing (Eng). Guilford Press, New York, p. 159.

McGarigal, K., 2015. FRAGSTATS HELP accessed. http://www.umass.edu/landeco/resea rch/fragstats/documents/fragstats.help.4.2.pdf. (Accessed 14 September 2017).

McGee, T.G., 2002. Reconstructing the southeast asian city in an era of volatile globalization. In: Bunnell, T., Drummond, L.B.W., Ho, K.C. (Eds.), Critical Reflections on Cities in Southeast Asia. Times Academic Press, Singapore, pp. 31–53.

Nguyen, T.B., Samsura, D.A.A., van der Krabben, E., Le, A.-D., 2016. Saigon-Ho Chi Minh city. Cities 50, 16–27.

Ottinger, M., Clauss, K., Kuenzer, C., 2017. Large-scale Assessment of coastal aquaculture ponds with sentinel-1 time series data. Rem. Sens. 9 (5), 440.

Ottinger, M., Clauss, K., Kuenzer, C., 2018. Opportunities and challenges for the estimation of aquaculture production based on earth observation data. Rem. Sens. 10 (7), 1076.

Pham, V.C., 1999. Bewertung von Bodenerosion und Eignungsflächen für Reisanbau im tropischen Vietnam mit Hilfe von Fernerkundungs- und GIS-Techniken (ger). Zugl. Freie Univ., Berlin. Diss, 1998, 1. Aufl. ed. Wiss.-und-Technik-Verl., Berlin, 129 pp.

Phoung Chau, N.T., 2013. The Socioeconomic Impact Assessment of Climate Change in Ho Chi Minh City. Dissertation, Cottbus.

Piekarczyk, J., 2014. Application of remote sensing in agriculture. Geoinf. Pol. 13 (1).

Qi, J., Chehbouni, A., Huete, A.R., Kerr, Y.H., Sorooshian, S., 1994. A modified soil adjusted vegetation index. Rem. Sens. Environ. 48 (2), 119–126.

Rowcroft, P., 2008. Frontiers of change: the reasons behind land-use change in the Mekong Basin (eng). Ambio 37 (3), 213–218.

Rutten, M., van Dijk, M., van Rooij, W., Hilderink, H., 2014. Land use dynamics, climate change, and food security in Vietnam: a global-to-local modeling approach. World Dev. 59, 29–46.

Saaty, T.L., 1994. Fundamentals of Decision Making and Priority Theory with the Analytic Hierarchy Process (Eng), first ed. RWS Publications, Pittsburgh, PA, p. 527.

Saaty, T.L., 2008. Decision making with the analytic hierarchy process. Int. J. Serv. Sci. 1 (1), 83–98.

Sobrino, J.A., Jiménez-Muñoz, J.C., Paolini, L., 2004. Land surface temperature retrieval from LANDSAT TM 5. Rem. Sens. Environ. 90 (4), 434–440.

Son, N.-T., Chen, C.-F., Chen, C.-R., Thanh, B.-X., Vuong, T.-H., 2017. Assessment of urbanization and urban heat islands in Ho Chi Minh City, Vietnam using Landsat data. Sustai. Cities Soc. 30, 150–161.

Statistical Office HCMC, 2015b. Agriculture accessed. http://www.pso.hochiminhcity.g ov.vn/web/guest/niengiamthongke-nam2015. (Accessed 31 August 2018).

Statistical Office HCMC, 2015a. Population and Labour accessed. http://www.pso.hochi minhcity.gov.vn/web/guest/niengiamthongke-nam2015. (Accessed 31 August 2018).

Storch, H., Downes, N.K., 2011. A scenario-based approach to assess Ho Chi Minh City's urban development strategies against the impact of climate change. Cities 28 (6), 517–526.

Storch, H., Downes, N.K., Goedecke, M., Katzschner, L., Burghardt, R., van Nguyen, Thi Cam, Dao Anh, K., Nguyen Van, P., 2012. Land-use Planning Recommendations:

Adaption Strategies for a Changing Climate in Ho Chi Minh City, Vietnam: Summary for Decision-Makers, Cottbus, p. 65 Bl.

Syrbe, R.U., Hou, W., Grunewald, K., Mathey, Juliane, 2017. How green area our cities? Green space provision in urban areas. In: Grunewald, K., Li, J., Xie, G. (Eds.), Towards Green Cities: Urban Biodiversity and Ecosystem Services in China and Germany, first ed. Springer International Publishing, Cham, pp. 86–98.

Thinh, N.X., Vogel, R., 2007. Application of the analytic hierarchy process in the multiple criteria decision analysis of retention areas for flood risk management. In: Hryniewicz, O., Studziński, J., Szediw, A. (Eds.), Environmental Informatics and Systems Research: EnviroInfo Warsaw 2007 ; the 21st International Conference on "Informatics for Environmental Protection", Warsaw, Poland. Shaker, Aachen, pp. 675–682 [September 12 - 14, 2007].

Thinh, N.X., Walz, U., Schanze, J., Ferencsik, I., Göncz, A., 2004. GIS-based multiple criteria decision analysis and optimization for land suitability evaluation. In: Wittmann, J., Wieland, R. (Eds.), Simulation in Umwelt- und Geowissenschaften. Shaker Verlag, pp. 208–223.

Tran, H., Tran, T., Kervyn, M., 2015. Dynamics of land cover/land use changes in the Mekong Delta, 1973–2011: a remote sensing analysis of the tran van thoi district, Ca mau province, Vietnam. Rem. Sens. 7 (3), 2899–2925.

Turner, B.L., Skole, D., Sanderson, S., Fischer, G., Fresco, L., Leemans, R., 1995. Land-Use and Land-Cover Change: science/research plan: IGBP Report No. 35, HDP Report Nr. 7, Stockholm und Geneva. http://millenniumassessment.org/documents/IGBP _report_35-LUCC.pdf.

United States Geoloical Survey (USGS), 2013. Landsat - A Global Land-Imaging Mission, p. 4 accessed. http://pubs.usgs.gov/fs/2012/3072/fs2012-3072.pdf. (Accessed 30 November 2016).

USGS, 2016. Landsat 8 (L8) Data Users Handbook accessed. https://landsat.usgs.gov/sit es/default/files/documents/Landsat8DataUsersHandbook.pdf. (Accessed 13 September 2017).

van Tran, T., Ha, D.X.B., 2007. Urban land cover change through development of imperviousness in Ho Chi Minh City, Vietnam. Asian Conf. Rem. Sens. (ACRS) 1, 211–217.

Vietnam National Assembly, 2017. Resolution No. 54/2017/QH14.

Vu, M.H., Kawashima, H., 2017. Effects of urban expansion on suburban farmers?: livelihood in Vietnam: a comparative analysis of Ho Chi Minh city and Hanoi. Habitat Int. 65, 49–58.

Vu, T.-T., Thy, P.T.M., Nguyen, L.Đ., 2018. Multiscale remote sensing of urbanization in Ho Chi Minh city, Vietnam - a focused study of the south. Appl. Geogr. 92, 168–181.

Waffle, A.D., Corry, R.C., Gillespie, T.J., Brown, R.D., 2017. Urban heat islands as agricultural opportunities: an innovative approach. Landsc. Urban Plan. 161, 103–114.

Wang, F., Qin, Z., Song, C., Tu, L., Karnieli, A., Zhao, S., 2015. An improved mono-window algorithm for land surface temperature retrieval from Landsat 8 thermal infrared sensor data. Rem. Sens. 7 (4), 4268–4289.

Xu, H., 2006. Modification of normalised difference water index (NDWI) to enhance open water features in remotely sensed imagery. Int. J. Remote Sens. 27 (14), 3025–3033.

Yalew, S.G., van Griensven, A., Mul, M.L., van der Zaag, P., 2016. Land suitability analysis for agriculture in the Abbay basin using remote sensing, GIS and AHP techniques. Model. Earth Syst. Environ. 2 (2), 879.

Zeleny, M. (Ed.), 1976. Multiple Criteria Decision Making: Kyoto, 1975 (Eng). Springer, Berlin, p. 345.

Zhang, T., Li, Q., Yang, X., Zhou, C., Su, F., 2010. Automatic mapping aquaculture in coastal zone from TM imagery with OBIA approach. In: Liu, Y. (Ed.), 18th International Conference on Geoinformatics, 2010: 18 - 20 June 2010, Beijing, China. IEEE, Piscataway, NJ, pp. 1–4.